Digital images of a set of bright shapley ames disk galaxies from San Pedro Mártir glass plates[i]

R. Díaz-Hernández and J.A. García-Barreto
Instituto de Astronomía, Universidad Nacional Autónoma de México,
Apartado Postal 70-264 México, D.F. 04510, México,
e-mail: rdiaz@astroscu.unam.mx; tony@astroscu.unam.mx

M.A. Moreno-Corral
Instituto de Astronomía, Observatorio Astronómico Nacional,
Km. 103, Carretera Tijuana - Ensenada, Ensenada, B.C.,
Apartado Postal 877, 22860 México.

Recibido el 1 de agosto de 2008; aceptado el 24 de noviembre de 2008

Optical digital images of a set of Shapley Ames disk galaxies are presented. The images were taken originally on glass plates sensitive to blue light, namely, 103aO. The observations on glass plates were obtained mainly to study peculiar circumnuclear structures, crooked spiral arms, peculiar morphology and the identificatio of possible companions. The glass plates have been scanned and astrometry has been performed in order to determine the position of the brightest central region (compact nucleus) of each galaxy.

Keywords: Galaxies: spiral; astrometry; galaxies: individual (NGC 2997; NGC 3359; NGC 3627; NGC 4178; NGC 4245; NGC 4314; NGC 5194; NGC 5248; NGC 5383; NGC 5595; NGC 5597).

Se presentan imágenes digitales de un conjunto de galaxias de disco del catálogo Shapley Ames de galaxias cercanas. Las imágenes fueron tomadas originalmente en placas fotográfica de vidrio usando emulsión sensible a la región azul del espectro llamada 103aO. Las observaciones de las placas de vidrio fueron obtenidas principalmente para el estudio de estructuras circunnucleares peculiares, brazos espirales torcidos, morfología peculiar y la identificac ón de posibles compañeras. Las placas de vidrio han sido digitalizadas y se les ha realizado astrometría con la finalida de determinar la posición de la región central más brillante (núcleo compacto) de cada galaxia.

Descriptores: Galaxias: espirales; astrometría; galaxias: individuales (NGC 2997; NGC 3359; NGC 3627; NGC 4178; NGC 4245; NGC 4314; NGC 5194; NGC 5248; NGC 5383; NGC 5595; NGC 5597).

PACS: 98.52.Nr; 98.62.Js; 98.62.Tc .

1. Introduction

As found in the book *The Realm of the Nebulæ* [1] (...science is the one human activity that is truly progressive. This remarkable attribute of science deals with judgements concerning which it is possible to obtain universal agreement; agreement is secured by means of observation and experiment...) In the early eighteen century the astronomical term *nebulæ* was the term for permanent, cloudy patches in the sky that are beyond the limits of the solar system. Today, the term *nebulæ* is used for two quite different kinds of astronomical bodies. On the one hand are the clouds of dust and gas called *galactic nebulæ*. On the other hand are what are now recognized as independent stellar systems scattered throughout space beyond the limits of the galactic system. These have been called *extragalactic nebulæ*, or alternatively *external galaxies*: the term *nebulæ* offers the values of tradition; the term *galaxies*, the glamour of romance.

Historically, galaxies have been studied mainly by optical photography. (Since 1907 the numbers of galaxies recorded on photographic plates have increased so rapidly.) [1]. Although the light from stars of present day disk galaxies is mainly in the near infrared, optical images still yield most of our information about galactic structure.

In this study we present digital images of glass plates that were obtained in April, 1986 and March, 1987 to observe a set of external galaxies. The purpose of the observing program was primarily to detect galaxies with circumnuclear structures peculiar disk or spiral arm morphology (as for example crooked arms or tidal arms) and nearby large scale companion galaxies in order to study the dynamics of each galaxy in the program. We chose a set of normal and barred galaxies. The glass plates were big enough (20 cm $\times$ 22 cm) to cover $\approx 1^\circ$ square but at the same time too big to make paper prints. Since at our Instituto de Astronomía we did not have a photodensitometer, we kept the glass plates in a safe place until we could digitized them. The time came when a sister research institute in Mexico, namely INAOE[ii], acquired a system for digitizing glass plates.

Glass plate surveys of the entire sky already exist. In the 1950's, the firs set of an all-sky survey was initiated, resulting in nearly 2000 exposures of the entire sky called the POSS (Palomar Observatory Sky Survey). With the availability of fine grained emulsion after 1970, it was decided to perform a second all-sky survey in the 1980's called the POSS-II [2]. Today the images of both surveys are available on line in databases. Another important work from glass plates is the digitization of the ESO Quick Blue Schmidt sur-

TABLE I. OAN San Pedro Mártir Glass Plates.

OAN-SPM Plate No.	Object	Date	H.A[1].	E.T[2].
135	NGC 5597	April 9/1986	-24m	90
137	NGC 2997	April 9/1986	-41m	120
138	NGC 4178	April 9/1986	—	30
140	NGC 3359	April 9/1986	+52m	60
141	NGC 4245	April 9/1986	+1h 38m	60
151	NGC 5383	Jun 1-2/1986	14h 02m	60
175	NGC 3627	March 27/1987	+0h 30m	45
177	NGC 4314	March 27/1987	-0h 8m	15
179	NGC 4314	March 27/1987	+0h 34m	25
181	NGC 5248	March 27/1987	+0h 58m	45
190	NGC 5194	March 28/1987	+0h 54m	35

[1] H. A. refers to hour angle at start time of observation; h stands for hours, m stands for minutes.

[2] E.T. refers to exposure time in minutes.

vey plates containing information on 14, 155 galaxies making the Catalog denominated ESO-Uppsala Galaxies [3].

The advantages of working with digital images include the following:

a) It is possible to make astrometric measurements within a fraction of a pixel. This is excellent for astronomy and provides high accuracy in the measurements which in turn are used to compute object coordinates. Astrometric measurements on original plates involve human intervention and require accuracy of fractions of a millimeter which is very hard to do by hand.

b) The use of computational algorithms to do astrometry on digital image allows the process to be semiautomatic, faster, and reliable, and

c) It is much easier to identify and fi possible errors in the original photographic plate such as geometric errors, rotation of the image in comparison to celestial north-south, etc.

The present work involves the digitization of the glass plates and the anchorage of equatorial coordinates for each galaxy, using point sources, namely stars, as references with known positions as reported in star catalogs. The images presented in this work are not calibrated in flux §2 describes an introduction to glass plates used in astronomical photography, §3 describes the process of digitization, §4 describes the astrometric calibration and the estimation of the plate constants when fittin with a polynomial, §5 gives short comments on individual galaxies and §6 describes our short conclusions.

2. Glass plates in astronomical photography[iii]

The photographic glass plates with emulsion 103aO in this work were used with the 2.1 m telescope from the Observatorio Astronómico Nacional at San Pedro Mártir (OAN-SPM), Baja California, Mexico, operated by the Instituto de Astronomía, UNAM to detect the blue light of a few nearby disk galaxies. The geographic position of the OAN-SPM is Longitude=115° 27′ 49″, West, Latitude=31° 02′ 39″ North, Altitude=2,800 meters. This telescope has a Ritchey-Chretien design, the secondary mirror has a f/7.5 ($\approx$ 13.0 $''/mm$), the limits in hour angle is 5.5^h, and the limit in DEC is less than +69° and greater than -40°.

The present study describes the work on 11 photographic glass plates 103 aO, which have a size of 8×19 inches. Table I list the main characteristics of these plates. Kodak 103aO emulsion was used for all these photographic plates. The developing process was done using the D-19 developer for 6 minutes.

The photographic glass plates must be stored taking into account different factors such as the humidity and temperature of the environment in the storage room. The storage position must be changed from time to time. Bad management of the storage would produce a non uniform shrink of the emulsion across the glass plate. These factors would introduce errors in the astrometric and photometric measurements. The plates in this study were kept and at a constant room temperature, for several years.

3. Digitization process of glass plates

For our glass plates to be usable for the analysis and possible further computer processing, a function $f(x, y)$ must be created from a glass plate. This process is called digitalization and f is a function of the x, y coordinates on the plate and intensity at each point. The digitalization of the space coordinate (x, y) is called "image sampling" and the amplitude digitalization is known under the quantificatio name of "grey levels". An image is described in a approximated form of $f(x, y)$ by a series of organized samples equally spaced in the form of an N×M matrix, where each element of the matrix is a discrete amount that represents what is commonly called a "digital image". Each element of the matrix is called an "image element" or "pixel" [4].

In this way, we digitized the photographic plates at the Instituto Nacional de Astrofísica, Optica y Electrónica (INAOE) in Puebla, México. We used a high resolution scanner EPSON Expression 1680 Professional Firewire with a fla bed. The main characteristic of this scanner is its transparency unit which makes it possible to scan glass plates (non-opaque negatives). The glass plate is placed on the surface of the scanner, with the emulsion facing the scanner fla bed.

The incident light crosses the plate; this light is reflecte by the transparency unit so that it is reflecte and caught by the detector of the scanner in order to obtain an intensity map from the plate. The light source is a Xenon gas cold cathode fluorescen lamp. The photoelectric device is an Epson Matrix CCD line sensor.

TABLE II. Reference stars in the image including Galaxy NGC 2997

Star No.	R.A. (J2000)[1]	Dec. (J2000)[1]	USNO	R.A.(J2000)	Dec. (J2000)
1	9:47:01.47	-30:50:51.9	0591-0230740	09:47:01.48	-30:50:51.0
2	9:44:31.37	-30:50:50.8	0591-0229668	09:44:31.39	-30:50:51.0
3	9:46:54.72	-31:09:37.9	0588-0232948	09:46:54.72	-31:09:37.5
4	9:44:21.11	-31:11:14.9	0588-0231743	09:44:21.07	-31:11:14.2
5	9:47:18.07	-31:21:10.8	0586-0231319	09:47:18.04	-31:21:11.1
6	9:44:56.27	-31:35:27.0	0584-0237743	09 44 56.27	-31 35 26.9
7	9:47:26.36	-31:21:32.9	0586-0231379	09:47:26.38	-31:21:32.7
		Galaxy NGC 2997			
G[2]	9:45:38.80	-31:11:26.7	- - - - - -	- - - - - -	- - - - - -

[1] Estimated positions after fittin the plate with an algorithm which includes a 2^{th} order polynomial; RA is given in hours, minutes and seconds of time and Dec is given in degrees, minutes and second of arc. Given the x, y position and their ecuatorial coordinates from USNO, output of the algorithm recalculates the positions for the reference stars in the field The 7 stars were selected as position references in order to determine the position of galaxy NGC 2997.

[2] The fitte position for the center of NGC 2997 agrees with the position given by Zacharias [7] [NOMAD Catalog, Zacharias+ 2005] α(J2000.0)= $09^h\ 45^m\ 38^s.78$, δ(J2000.0)=-31° 11′ 26″.6; the difference are $\Delta\alpha$(Zach-this work)=+-$0^s.02$; $\Delta\delta$(z-tw)= $-0''.1$.

TABLE III. Reference stars in the image including Galaxy NGC 3359

Star No.	R.A. (J2000)[1]	Dec. (J2000)[1]	USNO	R.A.(J2000)	Dec. (J2000)
1	10:48:14.49	+63:20:44.0	1533-0209967	10:48:14.45	+63:20:43.7
2	10:49:09.65	+63:15:13.4	1532-0226876	10:49:09.68	+63:15:13.4
3	10:47:41.55	+63:17:16.3	1532-0226775	10:47:41.59	+63:17:16.8
4	10:44:55.20	+63:10:01.0	1531-0228015	10:44:55.21	+63:10:00.6
5	10:45:31.90	+63:05:39.0	1530-0229333	10:45:31.95	+63:05:39.4
6	10:45:00.65	+62:59:08.0	1529-0233733	10:45:00.65	+62:59:07.8
7	10:47:00.02	+63:33:55.8	1535-0183044	10:47:00.02	+63:33:55.9
		Galaxy NGC 3359			
G[2]	10:46:36.80	+63:13:25.8	- - - - - -	- - - - - -	- - - - - - -

[1] Estimated positions after fittin the plate with an algorithm which includes a 4^{th} order polynomial; RA is given in hours, minutes and seconds of time and Dec is given in degrees, minutes and second of arc. The 7 stars were selected as position references in order to determine the position of galaxy NGC 3359.

[2] The fitte position for the center of NGC 3359 agrees with the position given by Zacharias [7] [NOMAD Catalog, Zacharias+ 2005] α(J2000.0)= $10^h 46^m 36^s.73$, δ(J2000.0)=+63° 13′ 25″.5; the differences are $\Delta\alpha$(Z-tw)=-$0^s.7$; $\Delta\delta$(Z-tw)= $-0''.3$.

Before digitizing a plate, one must firs clean it. This process is performed taking into account the fragile material of the plates. In the cleaning process isopropyl alcohol is used to remove fingerprints dust and any other impurities in the side plate without the emulsion. The side plate with the emulsion is cleaned with a fin bristle brush.

The scanner sampling resolution is 1600 dots per inch. One obtains a pixel size of ≈ 16 microns (0″.197) using the transparency (positive) mode. The dynamic range used is 16 bit. Each image has a size of 12105 × 15618 pixels. The fi nal fil size for each image is ≈360 Mb. The digitized image obtained could be stored in a variety of different formats, *i.e.* a tiff, jpeg or fits

The images were not calibrated in flux The reason is that the process to transform photographic plates to digital file is carried out through several steps. We would need a digital linearized image (Flat-Fielding image) in flu units since the photographic plate is not a linear element. The linearized image could be obtained by means of the characteristic emulsion curve mainly from sensitometric spots. In the case of point sources, such as stars, it is possible to do flu calibration, but we would not be able to establish an appropriate algorithm for calibrating extended objects, such as galaxies. One of the problems with extended objects is to compute the sum of the flu es at different areas of a galaxy after adequate background subtraction. We tried some basic algorithms but without good results.

4. Astrometric calibration

The invention of photography and its subsequent application to astrophysical research resulted in a revolution in astronomy. Some of the areas profoundly affected by astronomical photography are radial velocity measurements, proper

TABLE IV. Reference stars in the image including Galaxy NGC 3627

Star No.	R.A. (J2000)[1]	Dec. (J2000)[1]	USNO	R.A.(J2000)	Dec. (J2000)
1	11:20:08.07	+12:56:43.0	1029-0235639	11:20:08.08	+12:56:43.1
2	11:21:17.79	+13:16:14.1	1032-0214057	11:21:17.79	+13:16:14.2
3	11:19:53.65	+13:19:45.7	1033-0206100	11:19:53.64	+13:19:45.8
4	11:20:47.90	+12:58:44.7	1029-0235722	11:20:47.92	+12:58:44.4
5	11:21:06.76	+12:39:36.4	1026-0236800	11:21:06.76	+12:39:36.6
6	11:18:45.64	+12:43:36.3	1027-0244015	11:18:45.64	+12:43:36.6
		Galaxy NGC 3627			
G1[2]	11:20:14.97	+12:59:29.3	- - - - - -	- - - - - -	- - - - - -
G2[3]	11:18:56.00	+13:05:32.9	- - - - - -	- - - - - -	- - - - - -

[1] Estimated positions after fittin the plate with an algorithm which includes a 4^{th} order polynomial; RA is given in hours, minutes and seconds of time and Dec is given in degrees, minutes and second of arc. Given the x, y position and their ecuatorial coordinates from USNO, output of the algorithm recalculates the positions for the reference stars in the field The 6 stars were selected as position references in order to determine the position of galaxy NGC 3627.
[2] This object is the galaxy in the plate NGC 3627. The fitte position for the center of this galaxy agrees with the position given by Zacharias [7] [NOMAD Catalog, Zacharias+ 2005] α(J2000.0)=$11^h\ 20^m\ 14^s.99$, δ(J2000.0)=+12° 59′ 29″.8; the differences are $\Delta\alpha$(Z-tw)=+0^s.02; $\Delta\delta$(Z-tw)= +0″.5.
[3] This object is the nearby companion disk galaxy NGC 3623 with position given by Zacharias [7] [NOMAD Catalog, Zacharias+ 2005] α(J2000.0)=$11^h\ 18^m\ 55^s.90$ δ(J2000.0)=+13° 05′ 32″.3; the differences are $\Delta\alpha$(Z-tw)=-0^s.10; $\Delta\delta$(Z-tw)= −0″.6.

TABLE V. Reference stars in the image including Galaxy NGC 4178

Star No.	R.A. (J2000)[1]	Dec. (J2000)[1]	USNO	R.A.(J2000)	Dec. (J2000)
1	12:12:54.49	+10:49:29.4	1008-0201804	12:12:54.53	+10:49:29.5
2	12:12:45.13	+10:45:30.8	1007-0201589	12:12:45.13	+10:45:30.7
3	12:12:37.43	+10:42:18.4	1007-0201562	12:12:37.43	+10:42:18.5
4	12:11:58.33	+10:47:51.4	1007-0201422	12:11:58.32	+10:47:51.4
5	12:13:42.89	+10:49:39.8	1008-0202006	12:13:42.87	+10:49:39.8
6	12:11:17.47	+10:52:43.1	1008-0201413	12:11:17.47	+10:52:43.1
		Galaxy NGC 4178			
G[2]	12:12:46.32	+10:51:58.2	- - - - - -	- - - - - -	- - - - - -

[1] Estimated positions after fittin the plate with an algorithm which includes a 4^{th} order polynomial; RA is given in hours, minutes and seconds of time and Dec is given in degrees, minutes and second of arc. Given the x, y position and their ecuatorial coordinates from USNO, output of the algorithm recalculates the positions for the reference stars in the field The 6 stars were selected as position references in order to determine the position of galaxy NGC 4178.
[2] The fitte position for the center of NGC 4178 agrees with the position given by Zacharias [7] [NOMAD Catalog, Zacharias+ 2005] α(J2000.0)=$12^h\ 12^m\ 46^s.5$, δ(J2000.0)=+10° 51′ 58″.6; the differences are $\Delta\alpha$(Z-tw)=+0^s.18; $\Delta\delta$(Z-tw)= 0″.4.

motion studies, parallax determinations, chemical abundance analysis, galactic and extragalactic structure studies, various solar system topics, and photometry. Indeed almost all of early 20th century observational astrophysics was possible because of the capabilities of photography.

Advances in the detection and recording of optical light continue. For optical astrometry purposes from plates or CCD image the principles of analysis are fundamentally the same independent of the light detection and recording mechanism. From a digital (glass) plate or CCD image the equatorial position of a celestial object under study can be obtained if the positions of the point sources (stars) from a published catalog (*i.e.* USNO, [5]) are taken as reference points.

The ultimate usefulness of optical photography for astrometric purposes stems from the existence of a relationship between the object's equatorial coordinates, the equatorial coordinates of the optical axis of the telescope, and the rectangular coordinates of the image in the focal plane. In the ideal situation, the imaging system (telescope plus detector) projects a portion of the celestial sphere onto a plane via the gnomonic projection. In this perfect case, the photographic plate is equivalent to a pinhole camera, and the rectangular coordinates on the focal plane are known as "ideal standard coordinates". The usual symbols for them are ξ and η [6]. The ideal is never achieved in practice, and one uses an approximation to the ideal standard coordinates called "ideal

TABLE VI. Reference stars in the image including Galaxy NGC 4245

Star No.	R.A. (J2000)[1]	Dec. (J2000)[1]	USNO	R.A.(J2000)	Dec. (J2000)
1	12:18:17.78	+29:53:00.6	1198-0201046	12:18:17.76	+29:53:00.6
2	12:17:14.90	+29:37:49.3	1196-0199685	12:17:14.87	+29:37:49.4
3	12:17:45.66	+29:49:30.7	1198-0200958	12:17:45.67	+29:49:30.6
4	12:17:35.68	+29:49:56.5	1198-0200933	12:17:35.69	+29:49:56.4
5	12:17:15.50	+29:53:46.8	1198-0200895	12:17:15.53	+29:53:46.9
6	12:16:48.40	+29:53:27.1	1198-0200810	12:16:48.38	+29:53:27.0
7	12:16:33.66	+29:42:12.7	1197-0198688	12:16:33.66	+29:42:12.9
8	12:16:46.37	+29:35:11.7	1195-0197901	12:16:46.36	+29:35:11.9
9	12:16:37.75	+29:33:38.3	1195-0197876	12:16:37.77	+29:33:38.1
10	12:17:45.29	+29:26:16.9	1194-0198565	12:17:45.29	+29:26:17.0
11	12:18:13.14	+29:35:17.9	1195-0198123	12:18:13.15	+29:35:17.9
		Galaxy NGC 4245			
G[2]	12:17:36.82	+29:36:28.9	------	------	------

[1] Estimated positions after fittin the plate with an algorithm which includes a 4^{th} order polynomial; RA is given in hours, minutes and seconds of time and Dec is given in degrees, minutes and second of arc. iven the x, y position and their ecuatorial coordinates from USNO, output of the algorithm recalculates the positions or the reference stars in the field The 11 stars were selected as position references in order to determine the position of galaxy NGC 4245.

[2] The fitte position for the center of NGC 4245 agrees with the position given by Zacharias [7] [NOMAD Catalog, Zacharias+ 2005] α(J2000.0)=$12^h\ 17^m\ 36^s.80$, δ(J2000.0)=+29° 36′ 28″.9; the differences are $\Delta\alpha$(Z-tw)=+$0^s.02$; $\Delta\delta$(Z-tw)= 0″.0.

measured standard coordinates". The usual symbols for these are x and y. The mapping for the ideal standard coordinates to the measured standard coordinates is termed the "plate model" and the parameters of the plate model are known as "plate constants".

The results of photographic astrometry depends on our ability to project a portion of the celestial sphere onto a plane (in this case, the plate plane) and relate the resulting ideal standard coordinates to the measured standard coordinates. We made this assumption, and the firs task in our work is to relate ideal standard coordinates to the corresponding equatorial coordinates. So we start from ξ, η, α^* and δ^* to compute α and δ while from α, δ, α^* and δ^* one computes ξ and η. α^* and δ^* represent the equatorial coordinates of the tangential point, which is the position of observation given to the telescope when the plate was taken. Given a photograph of some portion of the celestial sphere that contains the images of several reference stars (for each we know α and δ from previous observations and in a catalog) and the celestial object of interest (the program object), we now seek a method of translating the measured rectangular coordinates for all of the imaged objects into equatorial coordinates for the program object . Each departure from the ideal imaging process results in deviations from the perfect relationship $\xi{=}x, \eta{=}y$. The following equation relates ξ to α, α^*, δ and δ^* [6]:

$$\frac{\xi}{f} = \frac{cot\delta \sin(\alpha - \alpha^*)}{\sin\delta^* + \cot\delta\cos\delta^*\cos(\alpha - \alpha^*)}, \qquad (1)$$

where f is the telescope focal length. If we assume that $f = 1$, we can obtain

$$\cot\delta\sin(\alpha-\alpha^*){=}\xi\sin\delta^* + \xi\cos\delta^*\cot\delta\cos(\alpha-\alpha^*). \qquad (2)$$

On the other hand, we can also write the following expression for the left hand side: [6]

$$\cot\delta\sin(\alpha-\alpha^*) = \xi\left[\sin\delta^* + \cos\delta^*\frac{1-\eta\tan\delta^*}{\eta+\tan\delta^*}\right], \qquad (3)$$

where

$$\frac{\eta}{f} = \frac{\cos\delta^* - \cot\delta\sin\delta^*\cos(\alpha-\alpha^*)}{\sin\delta^* + \cot\delta\cos\delta^*\cos(\alpha-\alpha^*)}. \qquad (4)$$

If we again assume that $f = 1$, we can obtain

$$\begin{aligned}\eta\sin\delta^* + \eta\cot\delta\cos\delta^*\cos(\alpha-\alpha^*)\\ = \cos\delta^* - \cot\delta\sin\delta^*\cos(\alpha-\alpha^*),\end{aligned} \qquad (5)$$

by associating terms

$$\cot\delta\cos(\alpha{-}\alpha^*)(\eta\cos\delta^*{+}\sin\delta^*){=}\cos\delta^*{-}\eta\sin\delta^*, \qquad (6)$$

and

$$\cot\delta\cos(\alpha-\alpha^*){=}\frac{\cos\delta^*{-}\eta\sin\delta^*}{\eta\cos\delta^*{+}\sin\delta^*}{=}\frac{1{-}\eta\tan\delta^*}{\eta{+}\tan\delta^*}. \qquad (7)$$

Finally, from (3) and (7) one obtains

$$\alpha = \tan^{-1}\left[\frac{\xi}{\cos\delta^* - \eta\sin\delta^*}\right] + \alpha^*, \qquad (8)$$

TABLE VII. Reference stars in the image including Galaxy NGC 4314

Star No.	R.A. (J2000)[1]	Dec. (J2000)[1]	USNO	R.A.(J2000)	Dec. (J2000)
1	12:22:26.39	+29:55:04.7	1199-0199560	12:22:26.41	+29:55:04.5
2	12:23:00.90	+30:00:00.2	1200-0200819	12:23:00.90	+30:00:00.1
3	12:23:21.13	+30:10:31.8	1201-0199366	12:23:21.89	+30:10:31.8
4	12:22:45.29	+30:18:38.7	1203-0200671	12:22:45.34	+30:18:38.8
5	12:22:13.88	+30:14:38.3	1202-0199243	12:22:13.86	+30:14:38.6
6	12:21:31.64	+30:11:00.7	1201-0199136	12:21:31.66	+30:11:00.4
7	12:21:41.83	+29:57:17.8	1199-0199479	12:21:41.83	+29:57:17.9
		Galaxy NGC 4314			
G[2]	12:22:32.10	+29:53:44.0	- - - - - -	- - - - - -	- - - - - -

[1] Estimated positions after fittin the plate with an algorithm which includes a 4^{th} order polynomial; RA is given in hours, minutes and seconds of time and Dec is given in degrees, minutes and second of arc. Given the x, y position and their ecuatorial coordinates from USNO, output of the algorithm recalculates the positions for the reference stars in the field The 7 stars were selected as position references in order to determine the position of galaxy NGC 4314.

[2] The fitte position for the center of NGC 4314 agrees with the position given by Zacharias [7] [NOMAD Catalog, Zacharias+ 2005] α(J2000.0)=$12^h\ 22^m\ 32^s.03$, δ(J2000.0)=+29° 53′ 43″.9; the differences are $\Delta\alpha$(Z-tw)=-$0^s.07$; $\Delta\delta$(Z-tw)= $-0''.1$.

TABLE VIII. Reference stars in the image including Galaxy NGC 5194

Star No.	R.A. (J2000)[1]	Dec. (J2000)[1]	USNO	R.A.(J2000)	Dec. (J2000)
1	13:30:14.93	+47:10:27.7	1371-0282523	13:30:14.93	+47:10:27.7
2	13:31:21.19	+47:08:09.7	1371-0282811	13:31:21.19	+47:08:09.3
3	13:28:31.83	+47:00:32.7	1370-0275066	13:28:31.80	+47:00:32.9
4	13:30:35.95	+46:59:50.3	1369-0259934	13:30:35.95	+46:59:50.3
5	13:30:34.06	+47:16:45.1	1372-0290450	13:30:34.03	+47:16:44.9
6	13:29:13.26	+47:14:16.1	1372-0290253	13:29:13.27	+47:14:16.6
7	13:29:26.05	+47:21:13.7	1373-0290750	13:29:26.04	+47:21:13.2
		Galaxy NGC 5194			
G[2]	13:29:52.10	+47:11:43.9	- - - - - -	- - - - - -	- - - - - -

[1] Estimated positions after fittin the plate with an algorithm which includes a 5^{th} order polynomial; RA is given in hours, minutes and seconds of time and Dec is given in degrees, minutes and second of arc. Given the x, y position and their ecuatorial coordinates from USNO, output of the algorithm recalculates the positions for the reference stars in the field The 7 stars were taken as position references in order to determine the position of galaxy NGC 5194.

[2] The fitte position for the center of NGC 5194 agrees with the position given by Zacharias [7] [NOMAD Catalog, Zacharias+ 2005] α(J2000.0)=$13^h\ 29^m\ 52^s.18$, δ(J2000.0)=+47° 11′ 42″.1; the differences are $\Delta\alpha$(Z-tw)=+$0^s.08$; $\Delta\delta$(Z-tw)= $-1''.8$.

and

$$\delta = \tan^{-1}\left[\frac{\sin\delta^* + \eta\cos\delta^*}{\sqrt{\xi^2 + (\cos\delta^* - \eta\sin\delta^*)^2}}\right]. \qquad (9)$$

The fina result is a mapping between ideal standard coordinates and measured standard coordinates whose parameters are known as "plate constants". Once the functional form of the mapping is known, a statistical adjustment, using the reference stars, determines estimates for the plate constants. The best estimates of the ideal standard coordinates for the program object can then be obtained and, after inverting the gnomonic projection, its equatorial coordinates can be computed.

In order to determine the plate constants in the chosen model, the plate coordinates are expressed as a polynomial:

$$x = \alpha_0 + \alpha_1\xi + \alpha_2\eta + \alpha_3\xi^2 + \alpha_4\xi\eta + \alpha_5\eta^2 + \alpha_6\xi^3 + \alpha_7\xi^2\eta + \alpha_8\xi\eta^2 + \alpha_9\eta^3... \qquad (10)$$

$$y = \alpha'_0 + \alpha'_1\eta + \alpha'_2\xi + \alpha'_3\eta^2 + \alpha'_4\eta\xi + \alpha'_5\xi^2 + \alpha'_6\eta^3 + \alpha'_7\eta^2\xi + \alpha'_8\eta\xi^2 + \alpha'_9\xi^3... \qquad (11)$$

The common uncertainties with photographic plates that should be taken into account when estimating plate constants are: translation error, rotation, nonperpendicularity of the axes, centering error, focal length error, decentering distortion, tilt, radial distortion, coma, differential astronomical refraction, and annual aberration [6].

TABLE IX. Reference stars in the image including Galaxy NGC 5248

Star No.	R.A. (J2000)[1]	Dec. (J2000)[1]	USNO	R.A.(J2000)	Dec. (J2000)
1	13:37:29.79	+8:51:28.5	0988-0234370	13:37:29.79	+08:51:28.2
2	13:37:34.48	+9:15:28.3	0992-0230083	13:37:34.48	+09:15:28.4
3	13:38:43.23	+9:11:12:2	0991-0232830	13:38:43.23	+09:11:12.2
4	13:37:13.63	+8:54:14.1	0989-0233952	13:37:13.63	+08:54:14.3
5	13:37:32.76	+8:46:36:8	0987-0237449	13:37:32.78	+08:46:36.9
6	13:38:34:29	+8:40:42.6	0986-0235909	13:38:34.25	+08:40:42.6
7	13:37:41:14	+8:34:20.7	0985-0234984	13:37:41.13	+08:34:20.7
8	13:36:03.86	+8:36:47.1	0986-0235511	13:36:03.89	+08:36:47.0
		Galaxy NGC 5248			
G[2]	13:37:32.22	+8:53:06.5	- - - - - -	- - - - - -	- - - - - -

[1] Estimated positions after fittin the plate with an algorithm which includes a 5^{th} order polynomial; RA is given in hours, minutes and seconds of time and Dec is given in degrees, minutes and second of arc. Given the x, y position and their ecuatorial coordinates from USNO, the output of the algorithm recalculates the positions for the reference stars in the field The 8 stars were selected as position references in order to determine the position of galaxy NGC 5248.

[2] This object is the galaxy in the plate NGC 5248. The fitte position for the center of this galaxy agrees with the position given by Zacharias [7] [NOMAD Catalog, Zacharias+ 2005] α(J2000.0)=$13^h\ 37^m\ 32^s.27$, δ(J2000.0)=+08° 53′ 06″.2; the differences are $\Delta\alpha$(Z-tw)=+$0^s.05$; $\Delta\delta$(Z-tw)= $0''.3$.

TABLE X. Reference stars in the image including Galaxy NGC 5383

Star No.	R.A. (J2000)[1]	Dec. (J2000)[1]	USNO	R.A.(J2000)	Dec. (J2000)
1	13:56:51.05	+41:53:04.5	1318-0270655	13:56:51.07	+41:53:04.5
2	13:57:57.72	+42:11:04.1	1321-0293364	13:57:57.14	+42 11 05.1
3	13:58:28:35	+42:01:42.4	1320-0284066	13:58:29.18	+42:01:42.5
4	13:55:50:22	+41:52:04.2	1318-0270493	13 55 50.22	+41:52:04.2
5	13:58:13.50	+41:38:19:4	1316-0254241	13:58:13.53	+41:38:19.4
6	13:56:07:35	+41:36:15:3	1316-0253970	13:56:07.36	+41:36:15.5
7	13:56:16.00	+41:55:14.4	1319-0278175	13 56 15.66	+41:55:14.7
		Galaxy NGC 5383			
G[2]	13:57:04.65	+41:50:45.19	- - - - - -	- - - - - -	- - - - - -

[1] Estimated positions after fittin the plate with an algorithm which includes a 4^{th} order polynomial; RA is given in hours, minutes and seconds of time and Dec is given in degrees, minutes and second of arc. Given the x, y position and their ecuatorial coordinates from USNO, output of the algorithm recalculates the positions for the reference stars in the field The 7 stars were selected as position references in order to determine the position of galaxy NGC 5383.

[2] The fitte position for the center of NGC 5383 agrees with the position given by Zacharias [7] [NOMAD Catalog, Zacharias+ 2005] α(J2000.0)=$13^h\ 57^m\ 04^s.70$, δ(J2000.0)=+41° 50′ 45″.2; the differences are $\Delta\alpha$(Z-tw)=+$0^s.05$; $\Delta\delta$(Z-tw)= $0''.01$.

4.1. Coordinate measurement in plates

The measurement of the coordinates (x, y) of astronomical objects on the digitized image from photography plates was made by means of a computer program. This program uses techniques of image segmentation to select the objects of interest. The program find the brightest region of objects of interest and determines its x, y position on the glass plate. A bright region is define as a region of interest whose intensity is greater than 3σ, where σ is the rms of blank sky.

4.2. Obtaining the equatorial coordinates of the disk galaxies

In order to perform astrometry of objects of interest, it is necessary to know their x and y position on the plate and their equatorial coordinates (α and δ). The equatorial coordinates of the reference stars were taken from the USNO B-1 catalog [5].

It is important to take into account the focal length of the telescope, and the observation date and period.

Although there is not a minimum of reference stars for a successful convergence of the astrometry algorithm, it is necessary to provide at least 5 reference stars. The order of the polynomial fi function depends on the number of stars used as reference, therefore for higher order terms $n + 2$ stars are needed, where n is the order of the polynomial.

There is not an absolute rule to select (isolated) reference stars from the glass plates. It is recommended reference star

TABLE XI. Reference stars in the image including Galaxy NGC 5597

Star No.	R.A. (J2000)[1]	Dec. (J2000)[1]	USNO	R.A.(J2000)	Dec. (J2000)
1	14:24:42.71	-16:40:48.6	0733-0303641	14:24:42.70	-16:40:48.7
2	14:24:37.32	-16:39:58.8	0733-0303620	14:24:37.34	-16:39:58.8
3	14:24:31.12	-16:39:19.5	0733-0303587	14:24:31.11	-16:39:19.6
4	14:24:37.86	-16:42:32.8	0732-0317867	14:24:37.86	-16:42:32.8
5	14:24:11.04	-16:48:35.9	0731-0327552	14:24:11.04	-16:48:36.0
6	14:24:06.49	-16:45:46.9	0732-0317679	14:24:06.49	-16:45:46.9
		Galaxy NGC 5597			
G1[2]	14:24:27.49	-16.45:45.9	- - - - - -	- - - - - -	- - - - - -
G2[3]	14:24:13.33	-16:43:21.6	- - - - - -	- - - - - -	- - - - - -

[1] Estimated positions after fittin the plate with an algorithm which includes a 4^{th} order polynomial; RA is given in hours, minutes and seconds of time and Dec is given in degrees, minutes and second of arc. The 8 stars were selected as position references in order to determine the position of galaxy NGC 5597.
[2] The fitte position for the center of NGC 5597 agrees with the position given by Zacharias [7] [NOMAD Catalog, Zacharias+ 2005] α(J2000.0)=$14^h\ 24^m\ 27^s.44$, δ(J2000.0)=-16° 45′ 46″.0; the differences are $\Delta\alpha(Z-\text{tw})$=-$0^s.05$; $\Delta\delta(Z-tw)=-0''.1$.
[3] This object is galaxy NGC 5595 with the position given by Zacharias [7] [NOMAD Catalog, Zacharias+ 2005] α(J2000.0)=$14^h\ 24^m\ 13^s.51$, δ(J2000.0)=-16° 43′ 21″.9; the differences are $\Delta\alpha$(Z-tw)=-$0^s.18$; $\Delta\delta$(Z-tw)= $+0''.3$.

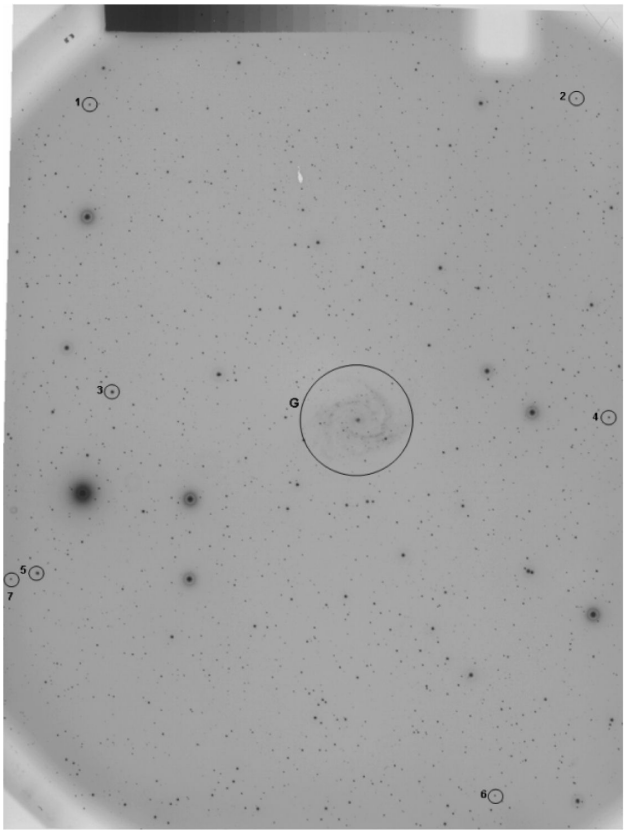

FIGURE 1. Scanned 103aO glass plate image in the region around NGC 2997. The objects labeled 1 to 7 are the stars chosen for the astrometry. NGC 2997 is labeled object G. The fiel is approximately $1° \times 1°$, the pixel size is $0''.197$. North is up, East is to the left.

be select from a region nearby (around) the studied galaxy and some reference stars from different regions far from it. In an ideal case it is recommended that one star be chosen from each corner, and at least one star close to the center of the image. The above is due to a variety of circumstances such as a lack of stars, saturated stars (never recommended to be taken as reference stars), or poor quality of the image (*i.e.* short exposures times, crowded fields etc.). A very important requirement is that reference stars must not be saturated and there must not be a very extensive object in the image, in order to determine the exact x and y position.

In this work, the number of reference stars for each analyzed image varies, *e.g.* in the glass plates with NGC 5597, NGC 3627 and 4178 6 reference stars were chosen to make

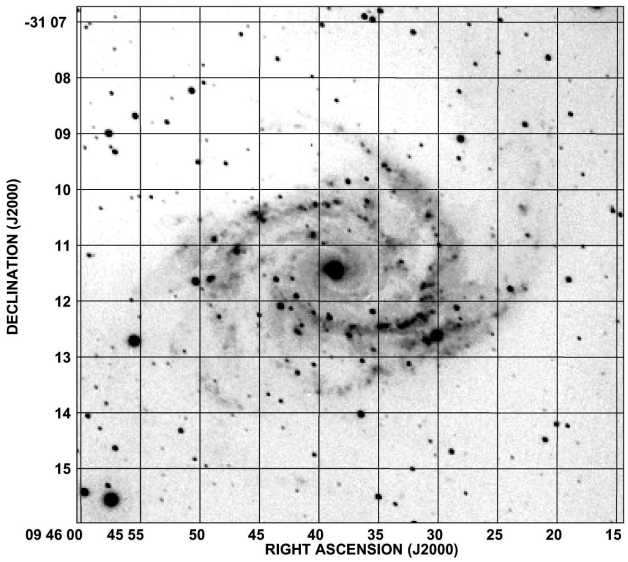

FIGURE 2. Close-up from Fig. 1 of NGC 2997, grey scale is proportional to surface brightness in arbitrary units (negative image: white sky and dark bright objects).

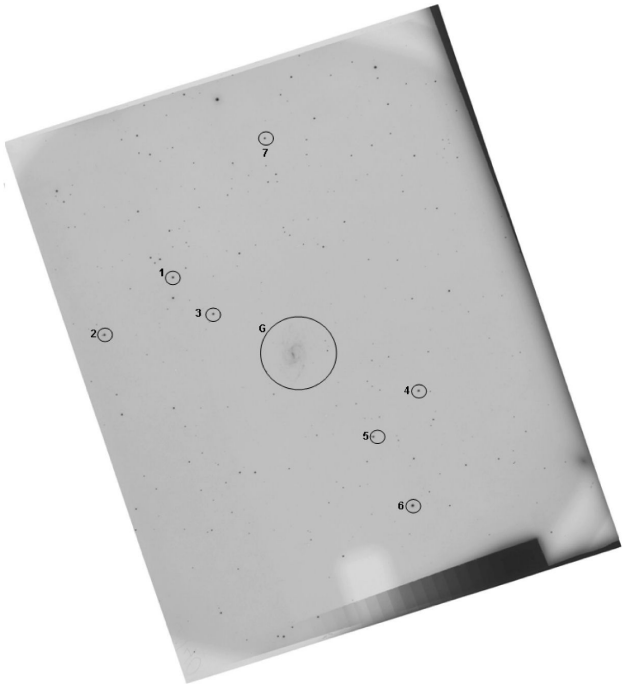

FIGURE 3. Scanned 103aO glass plate image in the fiel around disk galaxy NGC 3359. Seven stars were chosen as reference points for astrometry, labeled 1 though 7. Source labeled G is the galaxy NGC 3359. No nearby large scale galaxy is observed in this fiel near NGC 3359 and in fact it has no nearby large scale companion within 20 diameters [11]. The fiel size and orientation is the same as in Fig. 1.

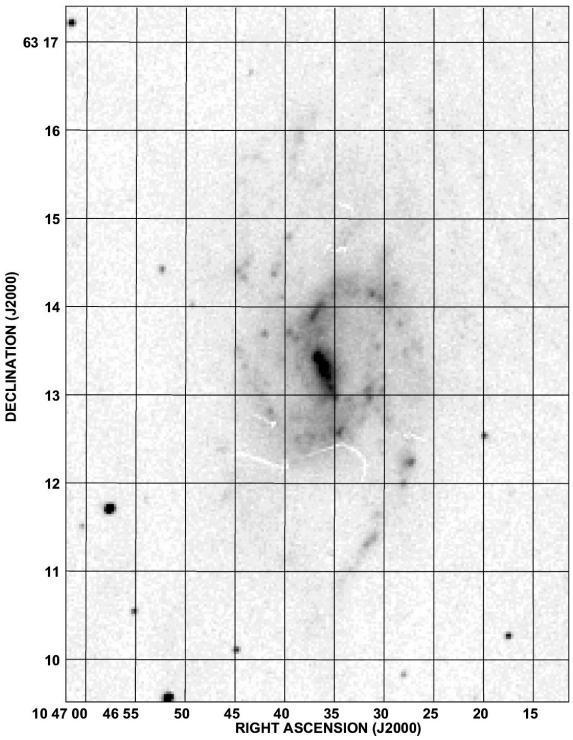

FIGURE 4. Close-up from Fig. 3 the disk galaxy with stellar bar NGC 3359; grey scale is proportional to surface brightness in arbitrary units (negative image: white sky and dark bright objects).

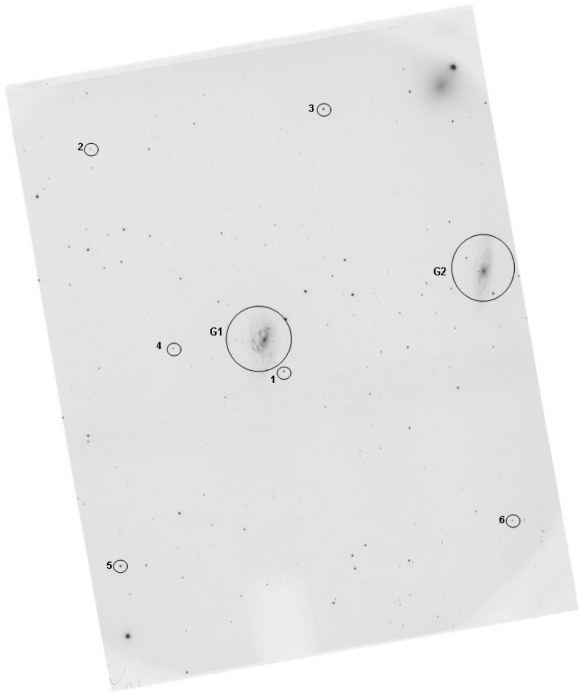

FIGURE 5. Scanned 103aO glass plate image in the fiel around disk galaxy NGC 3627. Six stars were selected as reference stars for astrometry, labeled 1 though 6; sources labeled G1 and G2 are the disk galaxies NGC 3627 and its nearby companion GC 3623 respectively. The fiel size and orientation is the same as in Fig. 1.

The order of the polynomial function is determined as a function of the best results of the calculated coordinates for each reference star; these calculated coordinates are compared to the coordinates from the catalog and thus the order that produces the minimum error is chosen.

The technique we have developed is capable not only of performing the equatorial coordinate identificatio of the galaxies under study, but it is also capable of calculating the equatorial coordinates for different objects on the glass plate image regardless of their physical position on the plate. The possible errors in the glass plate can be detected with this method and corrected in order to obtain the best fitting

The bootstrapped equatorial positions for the reference stars obtained after fittin polynomials on the plates agreed to within $< \pm 0^s.05$ and $< \pm 2''$.

The estimated equatorial positions for the galaxies observed were compared with the positions given by Zacharias *et al.*, [7]. They agreed within $< \pm 0^s.05$ and $< \pm 4''$, with NGC 4178 being the worst case, as seen in Tables II to XI.

5. Comments on individual objects

NGC 2997: The galaxy is classifie as Sc(s) I.3; the apparent blue magnitude is B_T=10.32 [8]. The total HI mass M=1.3 $\times$ $10^{10} M_\odot$, while the radial velocity in HI is 1084 kms^{-1} [9]. Visual inspection of the plate shows clearly the galaxy with no other galaxy in the field (see Fig. 1). The nucleus and the arms of the galaxy are clearly visible

(see Fig. 2). The arms are well defined but they seem to split into bright regions at their ends. Its equatorial coordinates have been calculated and listed in Table II. The string of star forming regions along NGC 2997 spiral arms on nearinfrared K-band images have been reported by Grosbøl, Dottori & Gredel [10].

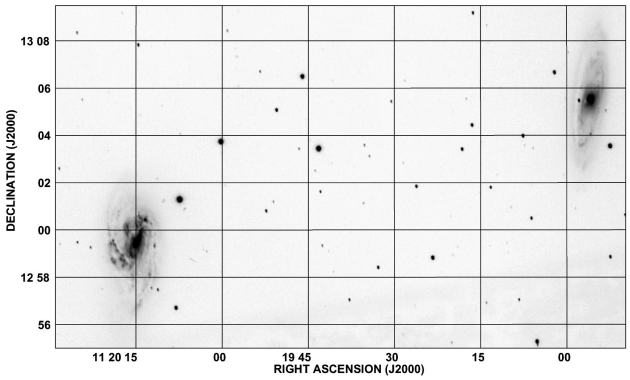

FIGURE 6. Close-up from Fig. 5 for the system of disks galaxies NGC 3627 and NGC 3623, grey scale is proportional to surface brightness in arbitrary units (negative image: white sky and dark bright objects). NGC 3627 (the program galaxy) lies to the east of this image; its companion NGC 3623 lies to the right (west on the sky) of this image.

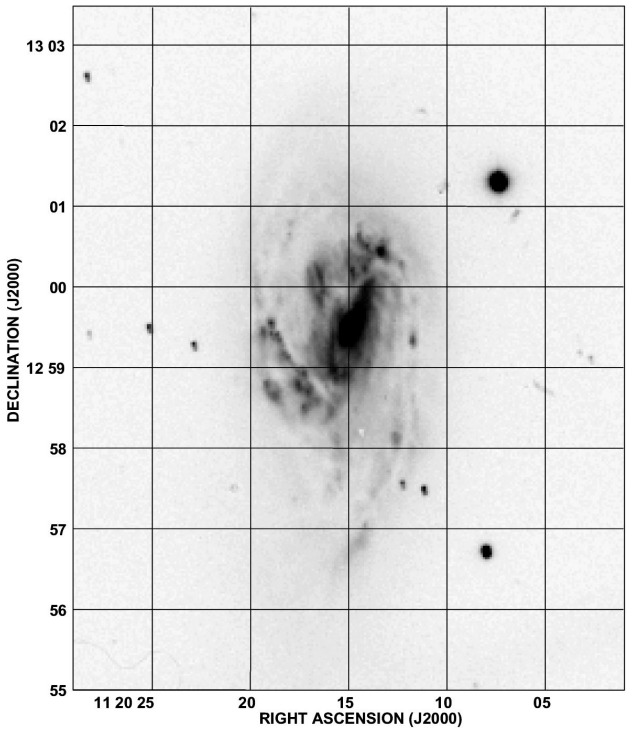

FIGURE 7. Close-up from Fig. 5 of NGC 3627; grey scale is proportional to surface brightness in arbitrary units (negative image: white sky and dark bright objects).

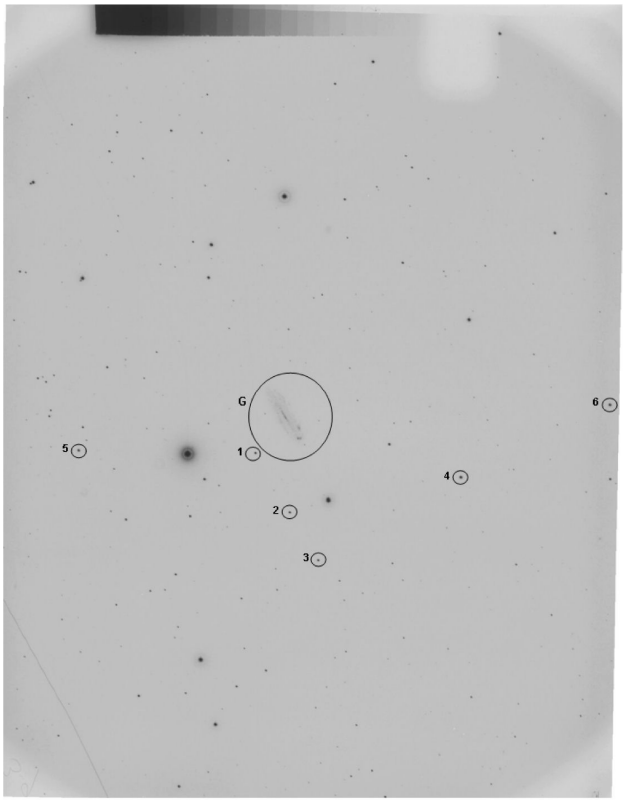

FIGURE 8. Scanned 103aO glass plate image in the fiel around disk galaxy NGC 4178. Six stars were selected as reference stars for astrometry, labeled 1 though 6; source labeled G is NGC 4178. The fiel size and orientation is the same as in Fig. 1.

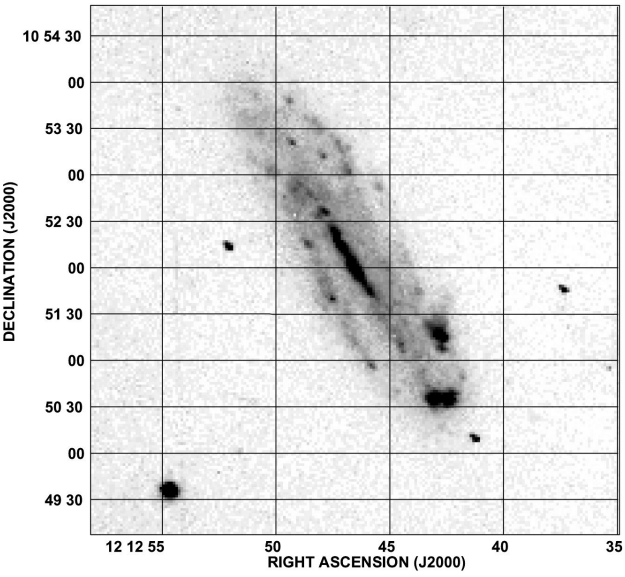

FIGURE 9. Close-up from Fig. 8 for the disk galaxies NGC 4178; grey scale is proportional to surface brightness in arbitrary units (negative image: white sky and dark bright objects). Notice the bright sources to the south-west.

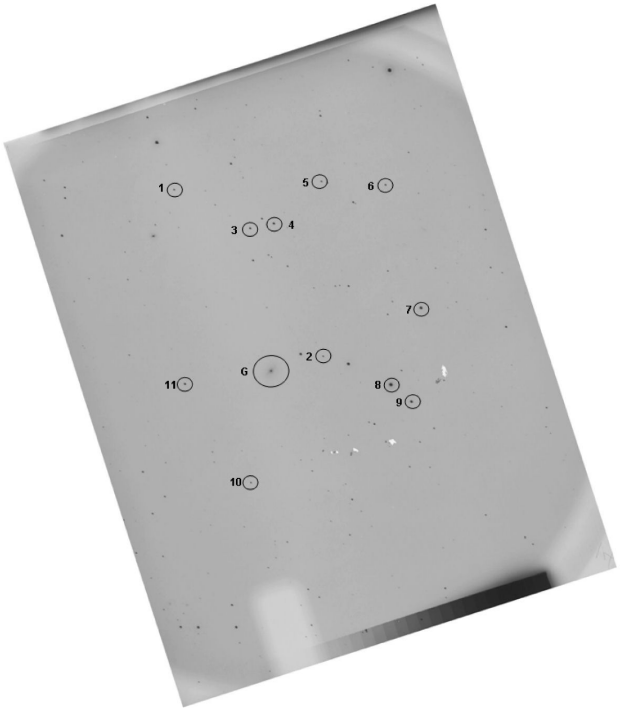

FIGURE 10. Scanned 103aO glass plate image in the fiel around NGC 4245. Eleven stars were selected as reference stars for astrometry, source labeled G is NGC 4245. The fiel size and orientation is the same as in Fig. 1.

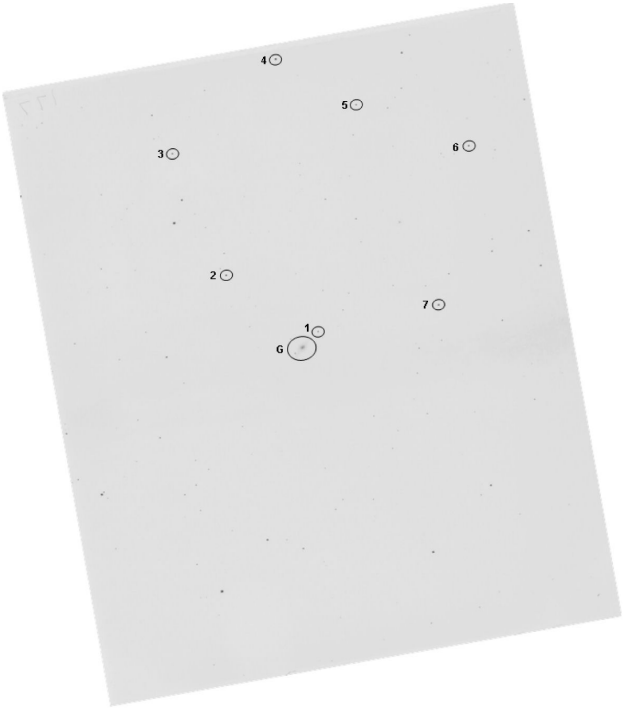

FIGURE 12. Scanned 103aO glass plate image in the fiel around disk galaxy with bar NGC 4314. Seven stars were selected as reference stars for astrometry, source labeled G is NGC 4314. The fiel size and orientation is the same as in Fig. 1.

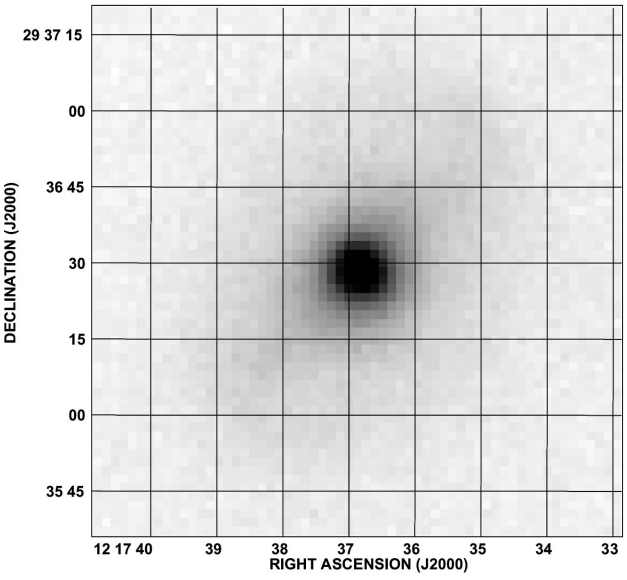

FIGURE 11. Close-up from Fig. 10 for NGC 4245; grey scale is proportional to surface brightness in arbitrary units (negative image: white sky and dark bright objects). This image shows a bright nucleus and weak emission from the disk.

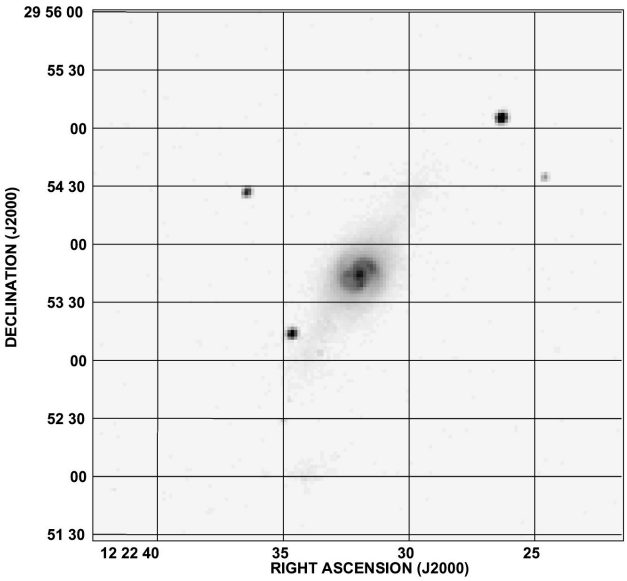

FIGURE 13. Close-up from Fig. 12 for the disk galaxy with bar NGC 4314; grey scale is proportional to surface brightness in arbitrary units (negative image: white sky and dark bright objects). This exposure shows a circumnuclear structure and a point as nucleus. Emission from the stellar bar is weak and no emission was detected from the spiral arms.

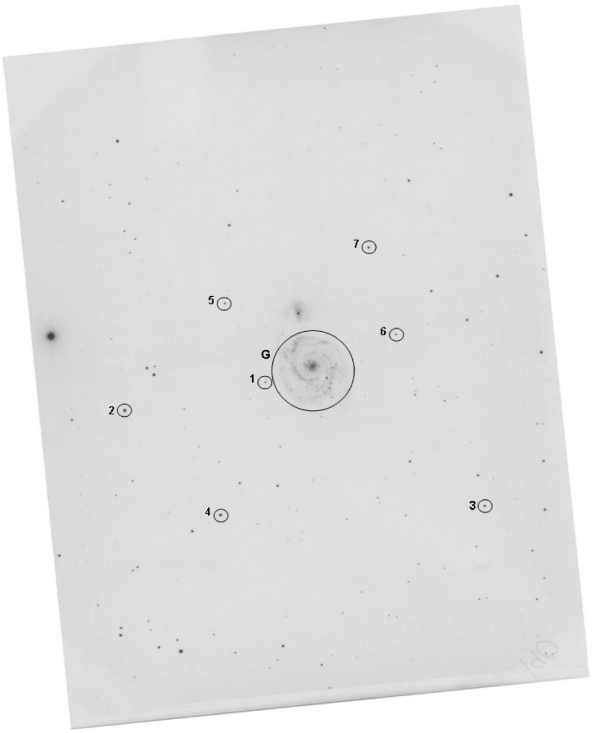

FIGURE 14. Scanned 103aO glass plate image in the fiel around disk galaxy NGC 5194 (M51). Seven stars were selected as reference stars for astrometry; source labeled G is NGC 5194 with its companion NGC 5195 to its north. The fiel size and orientation is the same as in Fig. 1.

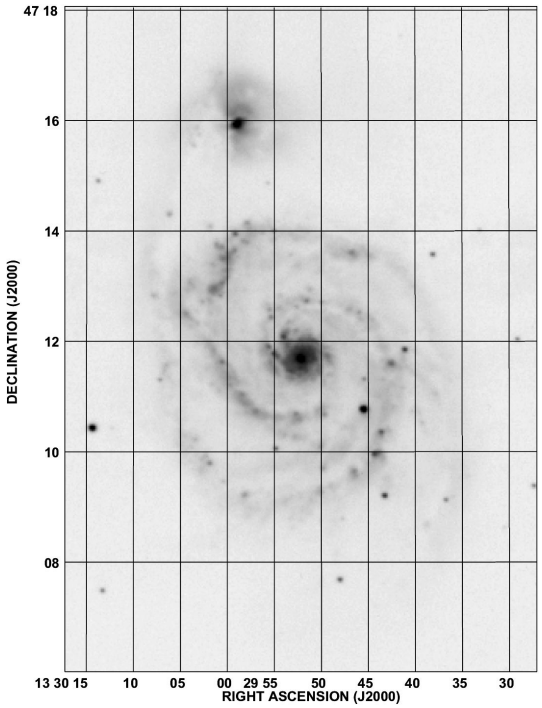

FIGURE 15. Close-up from Fig. 14 for the system of galaxies NGC 5194 (disk galaxy) and NGC 5195 (bar galaxy) to its north; grey scale is proportional to surface brightness in arbitrary units (negative image: white sky and dark bright objects). Notice the bright emission from the central region of NGC 5194 (M51) and the two bright regions to its north-east as starting region of spiral arms.

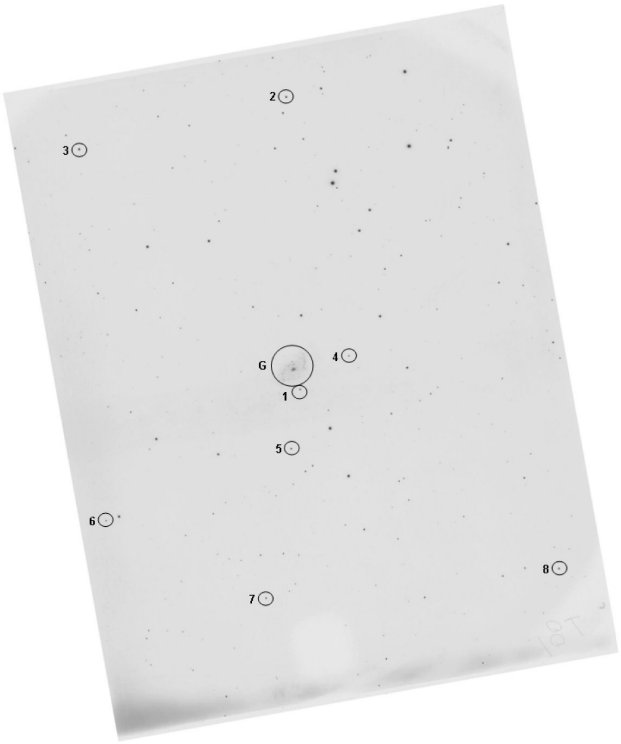

FIGURE 16. Scanned 103aO glass plate image in the fiel around disk galaxy NGC 5248. Eight stars were selected as reference stars for astrometry; source labeled G is NGC 5248. The fiel size and orientation is the same as in Fig. 1.

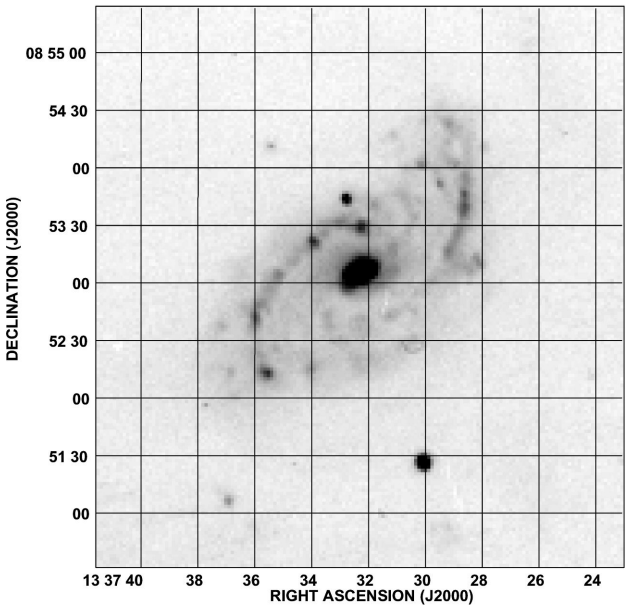

FIGURE 17. Close-up from Fig. 16 for the disk galaxy NGC 5248; grey scale is proportional to surface brightness in arbitrary units (negative image: white sky and dark bright objects). Notice the unresolved bright central region and the bright regions delineating the two spiral arms.

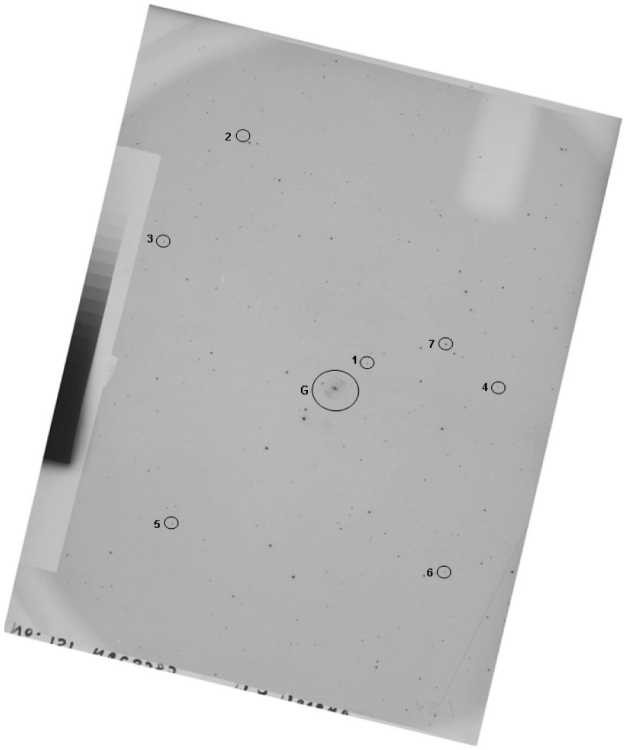

FIGURE 18. Scanned 103aO glass plate image in the fiel around disk galaxy with a bar NGC 5383. Seven stars were selected as reference stars for astrometry; source labeled G is NGC 5383 with its companion NGC 5383 to its north. The fiel size and orientation is the same as in Fig. 1.

FIGURE 20. Scanned 103aO glass plate image in the fiel around disk galaxy with a bar NGC 5597. Six stars were selected as reference stars for astrometry; source labeled G1 and G2 are NGC 5597 and its nearby companion to the north-west disk galaxy NGC 5595. The fiel size and orientation is the same as in Fig. 1.

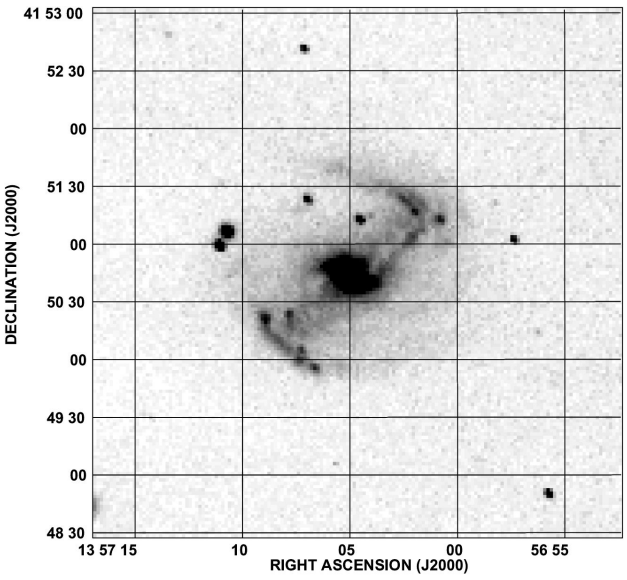

FIGURE 19. Close-up from Fig. 18 for the disk galaxy with a bar NGC 5383; grey scale is proportional to surface brightness in arbitrary units (negative image: white sky and dark bright objects). Notice the low surface brightness almost at the center of the bar and the bright central region.

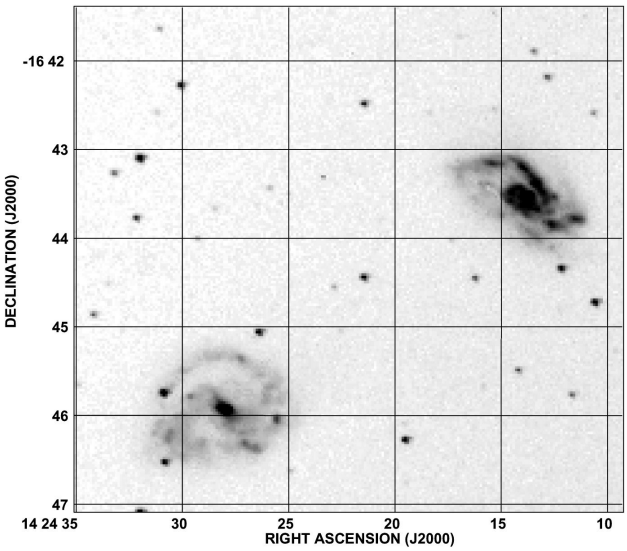

FIGURE 21. Close-up from Fig. 20 for the disk galaxy with a bar NGC 5597 (lower left on the image) and its nearby companion disk galaxy NGC 5595 (upper right on the image, north-west side of NGC 5597); grey scale is proportional to surface brightness in arbitrary units (negative image: white sky and dark bright objects). Notice the spiral arms in NGC 5597 facing NGC 5595: its spatial position might suggest a tidal interaction. NGC 5595 is the only large-scale companion of NGC 5597 within 20 diameters [11].

NGC 3359: The galaxy is classifie as SBc(s) I.8 pec, the apparent blue magnitude is B_T=10.99 [8]. The total HI mass M=6 $\times$ $10^9 M_\odot$, while the radial velocity in HI is 1008 kms^{-1} [9]. Visual inspection shows clearly the brightest regions of the bar with a high star concentration, and the two arms seem to be open and asymmetric. It is possible to observe dispersed light mainly from one of the arms. Figure 3 shows the plate image with NGC 3359 and no other galaxy in the fiel (in fact NGC 3359 has been shown to have no large-scale companions within a distance of 10 diameters projected on the sky [11]. Figure 4 shows the details for the light distribution in NGC 3359, the light narrow features are defects on the glass plate at the time of developing. Its far infrared (IRAS) flu es and radio continuum emission at 6.3 cm and 2.8 cm were reported by Garcia-Barreto *et al.* [12], its Hα and optical red continuum images have been also reported by Garcia-Barreto *et al.* [13]. Its magnetic fiel strength and polarization percentage have been reported by Beck *et al.* [14].

NGC 3627: The galaxy is classifie as Sb(s) II.2; the apparent blue magnitude is B_T=9.74 [8]. The total HI mass M=3 $\times$ $10^8 M_\odot$, while the radial velocity in HI is 740 kms^{-1} [9]. Visual inspection show clearly as the brightest region the central part of the galaxy and two asymmetric open arms with several regions of low surface brightness, most likely associated with dust lanes. NGC 3627 has a large scale companion to its north-west, namely NGC 3623 (see Fig. 6). Their spatial distribution of CO(J=1-0), has been reported by Sheth *et al.* [15].

NGC 4178: The galaxy is classifie as SBc(s) II, the apparent blue magnitude is B_T=11.89 [8]. The total HI mass M=5.1 $\times$ $10^9 M_\odot$, while the radial velocity in HI is 329 kms^{-1} [9]. It is possible to observe some of the bright regions in the arms and bright elongated emission from the central part of the galaxy. This galaxy has obviously no large scale spherical bulge around the compact nucleus. The ionized gas and stellar kinematics along NGC 4178's optical minor axis have been reported by Coccato *et al.* [16].

NGC 4245: The galaxy is classifie as SBa(s), the apparent blue magnitude is B_T=12.25 [8]. The total HI mass M=8 $\times$ $10^6 M_\odot$, while the radial velocity in HI is 890 kms^{-1} [17]. One can appreciate only a bright region, most likely the spherically symmetric bulge around the compact nucleus. The emission from the bar and disk is very weak. Upper limits on optical (Balmer) line flu es from its nucleus have been reported by Shield *et al.* [18]. Absorption-line strength maps obtained by SAURON have been reported by Peletier *et al.* [19].

NGC 4314: The galaxy is classifie as SBa(rs) pec, the apparent blue magnitude is B_T=11.35 [8]. The total HI mass is only M=4 $\times$ $10^6 M_\odot$, while the radial velocity in HI is 980 kms^{-1} [20], [16]. The image clearly shows a circumnuclear region and a bright nucleus of the galaxy. The circumnuclear structure is most likely the result of the dynamics under a non-axisymmetric gravitational potential, namely, near an Inner Lindblad Resonance shown by a multiwavelength study (radio continuum, optical continuum, distribution of molecular gas) [20]. Hα imaging of the circumnuclear structure has been also reported [13]. Nine large scale galaxy companions are within a projected distance of 20 diameters [11]. Absorption-line strength maps obtained by SAURON have been reported by Peletier *et al.* [19].

NGC 5194: The galaxy is classifie as Sbc(s) I-II, the apparent blue magnitude is B_T=8.98 [8]. The total HI mass M=9.2 $\times$ $10^8 M_\odot$, while the radial velocity in HI is 458 kms^{-1} [9]. Its nucleus is bright and, in this image, unresolved. Off the nucleus to the north east one can appreciate two bright regions associated with the starting regions of spiral arms. The innermost molecular gas CO(2-1) distribution has been reported by Scoville *et al.* [21]. High mass OB star formation through Hα and Paα observations has been reported by Scoville *et al.* [22].

NGC 5248: The galaxy is classifie as SBc(s) I-II, the apparent blue magnitude is B_T=10.80 [8]. The total HI mass M=3.9 $\times$ $10^9 M_\odot$, while the radial velocity in HI is 1152 kms^{-1} [9]. The nucleus is clearly define as well as the spiral arms. A new large scale stellar bar in NGC 5248 has been reported by Jogee *et al.* [23].

NGC 5383: The galaxy is classifie as SBc(s) I-II, the apparent blue magnitude is B_T=12.05 [8]. The total HI mass M=8 $\times$ $10^9 M_\odot$, while the radial velocity in HI is 2250 kms^{-1} [9]. The image shows clearly the central emission and the bar. Notice the lower surface brightness in the central part of the bar most likely delineating the shock regions. Massive star formation through its optical I and Hα images has been reported by Knapen *et al.* [24].

NGC 5595: The galaxy is classifie as Sc(s) II; the apparent blue magnitude is B_T=12.69 [8]. The total HI mass M=7.8 $\times$ $10^9 M_\odot$, while the radial velocity in HI is 2691 kms^{-1} [9]. The brighter regions are the nucleus and the northen arm. NGC 5595 is the only large scale companion to the barred galaxy NGC 5597 (García-Barreto, Carrillo & Vera-Villamizar 2003). New HI observations have been reported in the HIPASS [25].

NGC 5597: The galaxy is classifie as SBc(s) II; the apparent blue magnitude is B_T=12.6 [8]. The heliocentric velocity is 2683 kms^{-1} [26]. The image clearly shows a bright central region. The bright north-west spiral arm suggest a tidal interaction with NGC 5595. I optical red continuum and Hα images have been reported in [13]. New HI observations have been reported in the HIPASS [25].

6. Conclusions

In this work we presented digital images of a set of nearby Shapley Ames disk galaxies that were observed and detected on glass plates in April 1986 and March 1987 at the 2.1 m optical telescope in the OAN San Pedro Mártir, Baja California, México operated by the Instituto de Astronomía, UNAM. Our purpose at that time was to select a set of disk galaxies, normal and barred, that could have the morphology peculiar to circumnuclear structures and/or nearby large scale galaxy companions and study their dynamics. Over the years

we have continued our study on barred galaxies based on their far-infrared (IRAS) flu es to search for nearby Shapley Ames galaxies as possible candidates for having circumnuclear structures.

In this work we were able to digitize the glass plates, fin the plate constants in order to perform astrometry, and were able to anchor the positions of the galaxies using several point sources, namely, stars as reference points with known equatorial coordinates from printed catalogs (USNO). The bootstrapped positions of reference stars depended on the order of the polynomial, but finall good positions were found within $< \pm 0^s.05$ and $< \pm 2''$.

Acknowledgments

JAG-B acknowledges partial financia support from DGAPA (UNAM, Mexico) grants INI107806 and IN112408.

---

i Based on observations from the 2.1m optical telescope in the Observatorio Astronómico Nacional (OAN) in San Pedro Mártir, Baja California, México.

ii Instituto Nacional de Astrofísica, Optica y Electrónica, in Tonanzintla, Puebla, México

iii The invention of the dry gelatine emulsion in the late 1870s provided a safe and convenient method for optical photography. Photography became established as an essential tool of astronomers and led to a wealth of new discoveries. Astronomical photographic techniques continued to improve over the following century. As telescopes became larger they became much more sensitive. Photography works as a result of a photochemical reaction between incident light (photons) and the emulsion or fil on which the photons land. In professional astronomy the emulsion is normally on a glass plate rather than on more fl xible acetate or polyester film Glass plates are more rigid so they cannot wrinkle like fil does. This is essential for accurate astrometric measurements. A photographic plate is coated with a photographic emulsion comprising small silver halide crystals suspended in gelatin. Incident photons can be absorbed by electrons in the valence band of silver halide molecules. The subsequent movement of electrons into the conduction band creates positive holes in the valence band. Slight impurities in the silver halides act as traps, immobilising the electrons to prevent them from recombining with holes. Silver ions can then be neutralised by these immobile electrons, forming silver atoms. These atoms in turn then capture other conduction electrons and ions in turn. What starts as a single silver atom can grow to few hundred silver atoms within a silver halide crystal. These specks of silver act as catalysts during the developing process so that the surrounding silver halide is rapidly reduced to pure silver. The photographic process is therefore a chemical reaction. In normal photography the image produced is a negative (white sky and dark bright objects) whose image when printed translates into a positive (dark sky and bright objects are white).

1. E. Hubble *The Realm of the Nebulae* (New Haven: Yale University Press 1936)
2. I.N. Reid, *et al. PASP* **103** (1991) 661.
3. A. Lauberts and A. Valentijn, *The Surface Photometry Catalog of the ESO-Uppsala Galaxies*, (Garching bei Münich, European Southern Observatory, 1989)
4. R.C. González and R.E. Woods, *Tratamiento Digital de Imágenes* (Wilmington: Addison-Wesley-Díaz de Santos 1996)p. 34.
5. D.G. Monet, S.E. Levine, and B. Canzian, *et al. AJ* **125** (2003) 984.
6. L.G. Taff, *Computational Spherical Astronomy* (New York: John Wiley & Sons 1981)
7. N. Zacharias *et al.*, *AAS* **205**(2004) 4815Z. http://webviz.u-strasbg.fr/viz-bin/VizieR
8. A. Sandage and G.A. Tammann, *A Revised Shapley-Ames Catalog of Bright Galaxies* (Washington D. C.: Carnegie Institution 1981)
9. W.K. Huchtmeier and O.-G. Richter, *General Catalog of HI Observations of Galaxies* (New York: Springer-Verlag 1989)
10. P. Grosbøl, H. Dottori, and R. Gredel, *A&A* **453** (2006) 25.
11. J.A. García-Barreto, R. Carrillo, and N. Vera-Villamizar, *AJ* **126** (2003) 1707.
12. J.A. García-Barreto, R. Carrillo, U. Klein, and M. Dahlem, *Rev.Mex.AA.* **25** (1993) 31.
13. J.A. García-Barreto, J. Franco, R. Carrillo, S. Venegas, and B. Escalante-Ramírez, *Rev.Mex.AA.* **32** (1996) 89.
14. R. Beck *et al.*, *A&A* **391** (2002) 83.
15. K. Sheth, S.N. Vogel, M.W. Regan, M.D. Thronley, and P.J. Teuben, *ApJ* **632** (2005) 217.
16. L. Coccato, E.M. Corsini, A. Pizella, and F. Bertola, *A&A* **440** (2005) 107.
17. J.A. García-Barreto, D. Downes, and W.K. Huchtmeier, *A&A* **288** (1994) 705.
18. J.C. Shields *et al.*, *ApJ* **654** (2007) 125.
19. R.F. Peletier *et al.*, *MNRAS* **379** (2007) 475.
20. J.A. García-Barreto, *et al.*, *A&A* **244** (1991) 257.
21. N.Z. Scoville, M.S. Yun, L. Armus, and H. Ford, *ApJ*, **493** (1998) L63.
22. N.Z. Scoville, *et al. AJ* **122** (2001) 3017.
23. S. Jogee *et al.*, *ApJ* **570** (2002) L55.
24. J.H. Knapen *et al.*, *A&A* **448** (2006) 489.
25. M.T. Doyle, M.J. Drinkwater, and D.J. Rohde, *et al.*, *MNRAS* **361** (2005) 34.
26. L.Y. Schweizer, *ApJS* **64** (1987) 411.